



UNITED NATIONS
UNIVERSITY

UNU-GTP

Geothermal Training Programme

Orkustofnun, Grensasvegur 9,
IS-108 Reykjavik, Iceland

Reports 2016
Number 25

RESISTIVITY SURVEYING IN GEOTHERMAL EXPLORATION WITH AN APPLICATION TO THE EYJAFJÖRDUR LOW-TEMPERATURE AREA, N-ICELAND

Sarantsetseg Lkhagvasuren

Institute of Astronomy and Geophysics

Mongolian Academy of Science

P.O. Box 152, Ulaanbaatar

MONGOLIA

sarantsetseg@iag.ac.mn

ABSTRACT

Geothermal exploration involves geology, geochemistry and geophysics. In geophysical exploration, resistivity surveying plays the most important role in delineating the reservoir. The parameters that control the geothermal system show a strong response to electrical resistivity. The resistivity methods that are mostly used in geothermal exploration in Iceland are TEM (Transient ElectroMagnetics) and MT (MagnetoTellurics). The application of these methods is discussed in this report together with an example from the Eyjafjörður low-temperature area in N-Iceland. The resulting resistivity cross-sections and resistivity depth slices show a shallow lying low-resistivity layer and a deep lying low-resistivity anomaly towards the end of the cross-sections. The result of this work has been compared with results from Flóvenz and Karlsdóttir (2000) which interpreted TEM data from the same area. The results are also compared with borehole data and stratigraphy.

1. INTRODUCTION

Geothermal manifestations are commonly seen along plate boundaries and faults. A good example is Iceland, which is sliced or crossed by the North America and Eurasian plate's boundary. Geothermal systems are controlled by temperature, pressure, porosity, permeability and chemical composition of the fluid. These parameters give a response to electrical resistivity. Because of this, resistivity methods are the most powerful method used to find and delineate geothermal areas. The resistivity model of the Eyjafjörður low-temperature geothermal area is presented through 1D joint inversion of the MT (magnetotelluric) and TEM (transient electromagnetic) data. This work includes the two parts. Firstly, the intention is to give a short introduction to geophysical exploration methods that are widely used in geothermal exploration. This might be useful for future geothermal exploration in Mongolia. Secondly, resistivity of rocks is discussed and why resistivity methods are the most beneficial ones in geophysical exploration. The main part of this project work is the application of the MT and TEM methods in exploration of low-temperature geothermal areas. In TEM, an electrical current is injected into a source loop and then turned off abruptly. Afterwards, voltage is registered in a receiver loop as a function of time. MT uses natural fluctuations of the Earth's electromagnetic field – the electric and magnetic fields are registered in orthogonal directions. Data processing gives an apparent resistivity curve and a

resistivity model of the subsurface is obtained from an inversion process. Finally, the model is used for geothermal interpretation. These methods have been used effectively in geothermal exploration in Iceland for decades. Finally, the theory and application of the MT and TEM methods, respectively, are explained.

2. GEOPHYSICAL METHODS IN GEOTHERMAL EXPLORATION

According to the origin of field source, geophysical methods are divided into two groups that are called natural field and artificial field (controlled source) methods or passive and active methods. The natural field methods utilize the gravitational, magnetic and electromagnetic field of the Earth, searching for local perturbations of these naturally occurring fields that may be caused by concealed geological features of economic or other interest (Kearey et al., 2002). Geophysical methods are often used in combination. The objective of geophysics is to locate or detect the presence of subsurface structures or bodies and determine their size, shape, depth and physical properties (density, velocity, porosity and so on).

2.1 Seismic surveying

Seismic waves transfer energy through the ground. There are two types of seismic waves, body waves and surface waves. According to the polarization of particles, body waves are classified into primary (P) waves and secondary (S) waves. Surface waves are called Rayleigh (R) waves and Love (L) waves. Seismic waves travel through the earth's interior and indicate different elastic properties of the rock and composition of the rock with different density through their velocities. Equations 1 and 2 show their relationship with density and elastic coefficients of the rock.

$$V_p = \sqrt{\frac{\lambda + 2\mu}{\rho}} = \sqrt{\frac{K + \frac{4}{3}\mu}{\rho}}; V_s = \sqrt{\frac{\mu}{\rho}} \quad (1)$$

where K = Bulk modulus (modulus of incompressibility), ratio of pressure change to relative volume change;
 μ = Shear modulus (modulus of rigidity), equal to 0 for molten rocks;
 ρ = Density (kg/m³);
 λ = Lamé parameter.

The V_p/V_s ratio can be expressed as a function of the Poisson's ratio (σ). Poisson's ratio can be measured from seismic wave arrivals:

$$\frac{V_p}{V_s} = \sqrt{\frac{2(1 - \sigma)}{1 - 2\sigma}} \quad (2)$$

In geothermal environment, Poisson's ratio is typically in the range of 0.25 to 0.3 for normally saturated rock (Hersir and Björnsson, 1991).

2.1.1 Active seismic surveying

Seismic surveying has developed within oil and gas exploration, coupled with development of advanced electronic and data technology. According to the source of the energy, seismic surveying is divided into two methods, active and passive seismics. According to the wave propagation path, they may be classified into reflection and refraction methods (Lucius et al., 2006). Except for oil and mineral exploration, seismic methods are used to determine the depth and lateral extent of layers, thickness and

volume of deposits, and thickness of overburden. Seismic surveys record the ground motion caused by a known source in a known location (Kearey et al., 2002) and also with known magnitude. In active seismic surveying, seismic waves are caused by a controlled source, explosion, drop hitter, hammer or air guns and propagate through the subsurface. In a homogeneous earth, energy transmits by seismic waves from the source in all directions. Gradually, the seismic wave attenuates. In a heterogeneous and layered earth, seismic waves refract, reflect, diffract, convert and transmit between rock layers. Seismic traces are recorded in geophones mostly at the surface. Geophones are detectors of the seismic waves and usually laid out on the ground along a straight line. The electrical signal from the geophones is converted into digital values using modular 12-, 24- or 48-channel, high resolution, signal-enhancement seismographs. Seismographs are often linked together to increase the number of geophones. Portable computers record seismic waveforms (Lucius et al., 2006). Using the travel times of the seismic waves, a velocity model of the subsurface is obtained.

Generally, seismic surveying is divided into refraction methods, which give good information about stratigraphy, faults, intrusions and geological structure (Hersir and Björnsson, 1991) and reflection method, which is the main exploration tool in oil and gas exploration and very well suited to detect in details the interior of the sedimentary basins. However, in volcanic areas, the reflection method is expensive and not properly used because of the lack of reflector boundary and scattering due to chaotic structures. If a geothermal system is emplaced in a sedimentary basin, it is applicable (Flóvenz et al., 2012).

2.1.2 Passive seismic surveying – Seismological methods

Seismology is the science that studies earthquakes and seismic waves that travel through and around the earth. Earthquakes are mighty manifestations of abrupt releases of strain energy accumulated during extensive time intervals in the upper part of the earth. Various types of seismic waves radiate from the earthquake to all directions through the earth's interior and are recorded at large distances by sensitive instruments placed on or near the earth's surface (Kulhanek, 1988). An earthquake is classified into tectonic earthquake, volcanic earthquake, etc. Earthquakes happen along plate boundaries, faults and fissures. Volcanic earthquakes frequently happen in a volcanically active zone. A volcanically active zone is certainly found in Iceland where many volcanic eruptions happen. Some of the volcanoes are still active while others are dormant. Seismic stations are installed around the island and in study areas. Time series data are recorded at the stations and transmitted to a data centre, where locations of earthquakes are determined automatically or manually.

The main parameters of the earthquake are the origin time (t_0), epicentre (φ, λ) which is the end point of the vertical line starting from the hypocentre, depth (h) and the magnitude which is the amount of energy that is released by the earthquake. The seismic velocity provides information on the physical properties and compositions of the earth's layers and discontinuities.

The P-wave velocity is always considerably higher than the S-wave velocity. In seismic surveying, compressional waves are mostly used (Burger et al., 2006). Passive seismic surveying is used to investigate the earth's internal structure and monitor the seismic activity in the area. Earthquakes are induced during geothermal exploitation. Effects of exploitation of a geothermal reservoir can be monitored through micro-seismic activity (Mariita, 2011). Sometimes it is hard to say what causes an earthquake. Was it natural or induced? Passive seismic methods are widely used in geothermal exploration and monitoring (Samaranayake, 2015).

2.2 Gravity surveying

The basic theory of gravity surveying is governed by the law of gravitation. According to Newton's law of gravitation, the gravity force is directly related to the masses, m_1 and m_2 and reversely related to the distance squared, r^2 between the two bodies as expressed in Equation 3:

$$F = G \frac{m_1 m_2}{r^2} \quad (3)$$

where G = The universal gravitational constant $G = 6.67 \cdot 10^{-11}$ [Nm^2/kg^2].

In gravity surveys, the gravitational acceleration [m/s^2] is measured. The average gravitational acceleration (gravity) at the surface of the earth is $g \approx 9.81 \text{ m/s}^2$. Gravity varies by rock density, elevation and the earth's movement. Gravity, g is same for all bodies at a given place on Earth. It is expressed by Equation 4 given by Galileo:

$$g = \frac{F}{m} = \frac{G M_{\text{earth}}}{r^2} \quad (4)$$

Density varies for different types of rocks in the earth (Hersir and Björnsson, 1991). Lateral density variations in the subsurface cause gravity anomalies (Kearey et al., 2002). Gravity is measured at one place relative to a reference base station. In order to obtain useful information from the observed data that shows subsurface density variations at each gravity station, the following corrections have to be applied on the gravity readings before interpretation:

- *Tidal correction* (g_M) – measured gravity has to be corrected for the tidal effects (attraction of moon and sun) and drift in the gravimeter.
- *Free air correction* (C_{FA}) – reduces the gravity field from the altitude of the measuring site to sea level. Most on-land surveys are done above sea level, therefore this correction increases the gravity reading.
- *Bouguer correction* (C_B) – removes the effect of the rock mass between the measuring site and sea level. This correction decreases the gravity reading.
- *Terrain correction* (C_T) – topography variations (mountains or valleys) near each station affect gravity. The correction is carried out by estimating the differences between the elevation of the station and its surrounding. Terrain correction always reduces the gravity reading: mass excess above the station (mountains) decreases the gravity reading and mass deficiencies below (valleys) lead to overcorrection in the Bouguer correction and must be corrected for in the terrain correction. Thus, terrain corrected reading will always be higher than the measured values.
- *Latitude correction* (g_N) – correction that accounts for Earth's elliptical shape and rotation. Remember the gravity increases when moving towards the poles.

Having done all these corrections, the corrected gravity anomaly is called Bouguer anomaly, Δg_B , and expressed as:

$$\Delta g_B = g_M + C_{FA} - C_B + C_T - g_N \quad (5)$$

These corrections are discussed e.g. in Kearey et al., 2002; Hersir and Björnsson, 1991; Lichoro, 2014. Gravity anomalies are created by the lateral density contrasts between a body of rock and its surroundings. Density $\Delta\rho$ is given in Equation 6:

$$\Delta\rho = \rho_1 - \rho_2 \quad (6)$$

In Bouguer and terrain corrections and interpretation of the gravity anomaly, knowledge of rock density plays an important role. Rock density depends on its composition and porosity (Kearey et al., 2002).

Gravity measurements are a typical structural method that is used to detect geological formations with different densities in geothermal areas (Hersir and Björnsson, 1991). In gravity surveying, subsurface geological investigation is carried out on the basis of variations in the earth's gravitational field generated by differences of density between subsurface rocks. Since, gravity decreases as elevation increases, the elevation of each station has to be measured with an error of not more than about 10 cm. Differential GPS provides sufficient accuracy of the elevation evaluation.

2.3 Magnetic surveying

The magnetic field of the earth is imagined like a field from a large bar magnet located near the centre of the earth, a dipole field. The magnetic field is created by fluid currents in the conductive outer core. The magnetic lines are almost vertical close to the poles and horizontal near the equator (Figure 1). The earth's magnetic field is not a pure dipole field but contains higher order pole component (80% dipole, 20% higher order poles). The magnetic field vectors around the earth are defined to point in the direction from south to north. Magnetic properties are different for the different rock types. The magnetic field B_0 can induce a magnetic field B_M (magnetization field) in a material, which is proportional to the undisturbed external field B_0 ($B_M = kB_0$):

$$B = B_M + B_0 = (1 + k)B_0 = \mu B_0 \quad (7)$$

where, $\mu = 1 + k$ is the magnetic permeability, which is the relative ability of a material to create a local magnetic field while k is the magnetic susceptibility.

Minerals are divided into paramagnetic ($0 < k < 10^{-5}$), diamagnetic where the susceptibility is smaller and has a negative value, ferrimagnetic ($k \approx 1-4$) and ferromagnetic ($k \approx 10^1-10^6$). The magnetic field at any point on the earth's surface is a vector quantity defined by its total intensity and direction. The total field vector, \mathbf{B} , is defined by its intensity, its inclination I , which is the angle the vector makes with a horizontal plane, and its declination D , which is the angle the horizontal component \mathbf{H} of the total-field vector makes with geographic north. This is demonstrated in Figure 1.

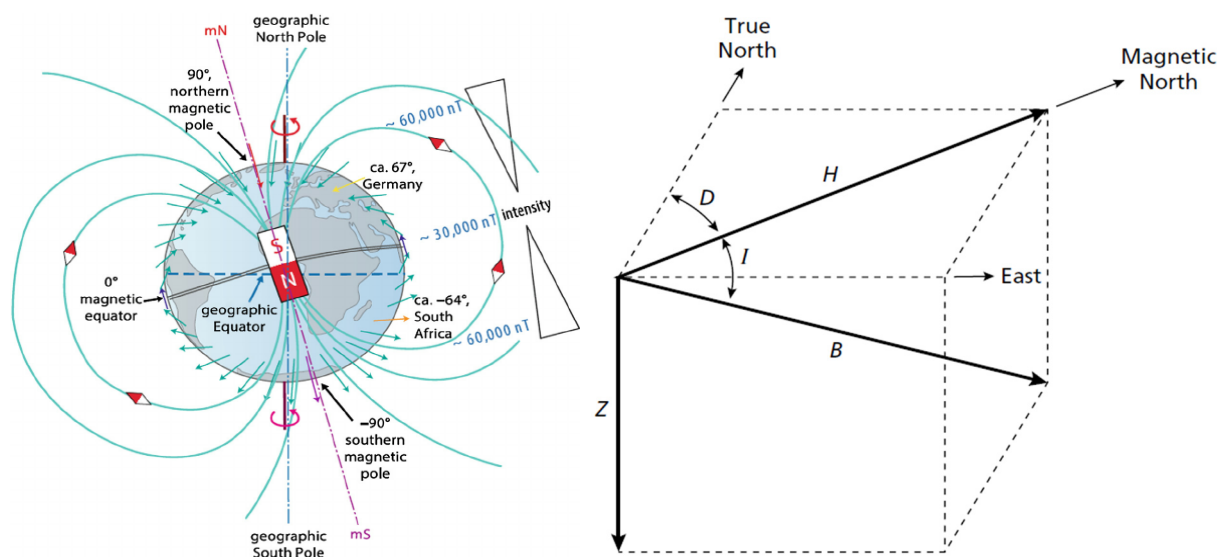


FIGURE 1: The elements of the earth's magnetic field: \mathbf{B} = total-field vector, \mathbf{H} = horizontal component, Z = vertical component, D = declination, and I = inclination (Kearey et al., 2002)

\mathbf{B} can be resolved into a vertical component Z and a horizontal component \mathbf{H} . The vertical plane containing \mathbf{F} , Z and \mathbf{H} is a magnetic meridian. \mathbf{H} can also be resolved into horizontal components directed toward geographic north H_x and geographic east H_y . Magnetic data collected at any points on the earth's surface can be displayed on a map of the world as contours of \mathbf{B} , I and D . Observations show that values of each element of the earth's magnetic field are permanently changing from hour to hour and from year to year. Magnetic surveying is an indirect method or structural method. Magnetics can be carried out on the ground and as aeromagnetics. Generally, magnetic methods are used to investigate regional geological structures.

Numerous aeromagnetic surveys have been completed over geothermal areas. Magnetic lows can be due to hydrothermal alteration of the geothermal system as confirmed by the surveys. Rocks lose their

magnetic properties at temperatures above Curie temperature (demagnetization). Detailed ground-magnetic surveys are used in Iceland to trace narrow linear features like dykes and faults where the basement is covered with soil (Hersir and Björnsson, 1991). Ground magnetic surveys are usually performed over relatively small and previously defined areas (Kearey et al., 2002).

2.4 Thermal methods

Thermal methods measure directly the temperature or heat of the geothermal system. There are basically the following four methods (Hersir and Björnsson, 1991):

- Temperature measurement; direct interpretation, mapping;
- Geothermal gradient that shows vertical variation of the temperature measured in soil or in shallow drillholes;
- Heat flow, that is calculated from the temperature gradient and thermal conductivity;
- Heat budget, that is done by measurement of spring flow and steam output and/or integrating areal heat flow.

The main heat exchange mechanisms are conduction and convection. Radiation in the earth does not play an important role for geothermal systems.

Conductional heat transfer is expressed by Equation 8:

$$Q_{cond} = -k \cdot \frac{\Delta T}{\Delta Z} \quad (8)$$

where k = Thermal conductivity (W/m °C), a constant of each material;
 $\Delta T/\Delta Z$ = Thermal gradient, defining temperature variations with depth, its distribution is very important to achieve an understanding and to delineate the geothermal resource on a regional and local scale.

Convection is heat transfer by motion of the mass, for example, natural circulation of hot water which is driven by a density gradient in the fluid.

2.5 Electrical resistivity of rocks - resistivity methods

2.5.1 Resistivity of rocks

The specific resistivity is defined by Ohm's law:

$$\mathbf{E} = \rho \mathbf{j} \quad (9)$$

where ρ = Resistivity (Ωm);
 \mathbf{E} = Electric field magnitude (V/m);
 \mathbf{j} = Current density (A/m^2).

The reciprocal value of resistivity is called conductivity $\sigma = 1/\rho$ (S/m or $1/\Omega\text{m}$).

Specific resistivity can also be defined as the ratio of the potential difference ΔV (V) to the current I (A), across a material which has a cross-sectional area of 1 m^2 and is 1 m long, or:

$$\rho = \frac{\Delta V A}{I L} = R \frac{A}{L} \quad (10)$$

where A = Cross-sectional area (m^2);
 L = Length (m).

Electrical conductivity in minerals takes place by the movement of electrons and ions. Conduction of electricity is mostly through groundwater present inside the pores of the rocks and along surface layers at the contact of rocks and solution (Hersir and Arnason, 2009).

2.5.2 Main factors affecting resistivity of water-bearing rocks

The specific resistivity of rocks is controlled by important parameters of the geothermal system like temperature, fluid type and salinity, porosity, the composition of the rocks, and the presence of alteration minerals.

Temperature plays a key role in altering the bulk resistivity of rock material. An aqueous environment present in the rock matrix contributes to this effect. The conductivity of pore fluid varies according to the formula given by Dakhnov (1962):

$$\sigma_w = \sigma_{w0}(1 + \alpha(T - T_0)) \quad (11)$$

where σ_w = Conductivity of the pore fluid (S/m) at temperature of T (°C);
 σ_{w0} = Conductivity of the pore fluid (S/m) at reference temperature of T_0 (°C);
 T = Temperature (°C);
 α = Temperature coefficient of resistivity, i.e. $\alpha = 0.023/^\circ\text{C}$ for $T_0 = 25^\circ\text{C}$.

Equation 11 is valid only for a temperature range of 0-200°C, the trend starts to reverse as the temperature increases further (Flóvenz et al., 2012).

Porosity and permeability: The fractional porosity ϕ_t of a material is defined as the ratio of the pore volume and the total volume of the material. There are primarily three types of porosity in rocks. Intergranular – pores are formed like spaces between particles in sediments and volcanic ash; joints - fractures – pores are formed by a net of fine fissures caused by tectonics or cooling of the rock; and vugular porosity – big and irregular pores have been formed because of the dissolution of material, especially in limestone (Flóvenz et al., 2012). The fractional porosity of rock is given in Equation 12:

$$\phi_t = \frac{V_\varphi}{V} \quad (12)$$

where ϕ_t = Fractional porosity;
 V_φ = Volume of the voids;
 V = Total volume of the material.

The porosity of the rock matrix and its pore connectivity or effective porosity has a large effect on resistivity. Porosity is described as primary where interstices are originally present in the rock matrix and secondary where void spaces are created as a result of external factors such as pressure and erosion (Todd and Mays, 2005). At this point, it is noteworthy to include Archie's law (Archie, 1942) which is an empirical law relating bulk resistivity to pore fluid resistivity and porosity as expressed in Equation 13:

$$\rho = \rho_w a \phi_t^{-n} \quad (13)$$

where ρ = Bulk (measured) resistivity (Ωm);
 ρ_w = Resistivity of the pore fluid (Ωm);
 a = An empirical parameter depending on porosity type, usually around 1;
 ϕ_t = Porosity in proportions of total volume;
 n = Cementing factor which is empirically determined; usually around 1-2.

Equation 13 may be simplified and expressed as shown in Equation 14:

$$\rho = \rho_w F \quad (14)$$

where F = The formation factor.

Permeability depends on porosity type and its connection. For example, a rock might be highly porous but the pores are isolated, then the rock would have no permeability and it will have high resistivity. The degree of interconnected pores within the rock is described as effective porosity. The characteristics of the host material, the viscosity and pressure of the fluid also affect the rate at which the fluid will flow (Lee et al., 2006).

Salinity is a measure of ions (salts) dissolved in water. The salinity in the groundwater varies and it affects the resistivity of the subsurface. The bulk resistivity of rocks in low-temperature geothermal areas is mostly controlled by the resistivity of the pore fluid, which is dependent on the salinity of the fluid. As the amount of dissolved solids in the pore fluid increases, the conductivity increases. The conductivity σ of a solution is a function of the salinity (the concentration of the ions) and the mobility of the ions in the solution. This is shown in Equation 15:

$$\sigma = \frac{1}{\rho} = F \cdot (c_1 q_1 m_1 + c_2 q_2 m_2 + \dots) \quad (15)$$

where σ = Conductivity (S/m);
 F = Faraday's number ($9.649 \cdot 10^4$ C/mole);
 c_i = Concentration of ions;
 q_i = Valence of ions;
 m_i = Mobility of the different ions.

2.5.3 DC methods

In the DC (direct current) resistivity method, a constant current I is injected into the earth through a pair of electrodes at the surface while the potential difference is measured at two receiver electrodes. The current creates a potential field which depends on the resistivity of the earth which can be inferred from the measured electric field (potential difference between the two electrodes) and the injected current. The most common DC methods are Schlumberger soundings, Head-on profiling, dipole soundings and profiling (Georgsson, 2009). Resistivity measurements are used to delineate geothermal systems, locate aquifers and sometimes to estimate porosity and physical conditions within the geothermal system. Electrical sounding methods reveal resistivity of the subsurface as a function of depth at a fixed location. Electrical profiling method can show lateral resistivity changes along a profile.

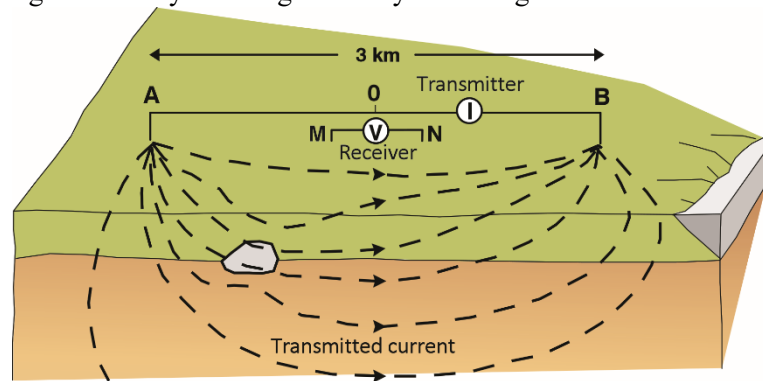
Schlumberger sounding: One type of electrode configuration of the DC method is the Schlumberger sounding, a conventional DC method which has been used widely (Georgsson and Karlsdóttir, 2007). In the Schlumberger configuration, two potential electrodes (M and N) and two current electrodes (A and B) are located along a straight line and connected to the voltage receiver and current transmitter, respectively. The distance between the A and B electrodes is symmetrically extended from the midpoint O (Hersir and Björnsson, 1991) to achieve greater depth of penetration. The setup of a Schlumberger sounding is illustrated in the Figure 2.

A current I is injected into the ground through electrode A, and the circuit is closed at electrode B. As the current travels through different conductivity media (Figure 2), the potential difference between the M and N electrodes is measured in the receiver. Apparent resistivity of the ground ρ_a is computed through Equation 16. Here is $AO = OB = S$ and $MO = ON = P$.

$$\rho_a = \frac{\pi S^2 - P^2}{2} \frac{\Delta V}{P I} \quad (16)$$

where ΔV = Potential difference;
 I = Injected current;
 $K = \frac{\pi S^2 - P^2}{2P}$ is a geometrical factor.

The apparent resistivity ρ_a is an average resistivity of the ground layers through which the current passes. The depth of penetration increases with increasing distance between the current electrodes and higher current must be injected. When the distance increases, potential difference decreases. The apparent resistivity is interpreted as specific resistivity and becomes a function of depth only applying 1D interpretation. If resistivity changes in one horizontal direction as well, 2D interpretation is needed.



The head-on profiling method can detect narrow near-vertical resistivity structures like faults, dykes and fractures. These structures are often correlated to upflow of geothermal fluid. The setup is the same as for Schlumberger soundings but it has an additional current electrode C placed far away from the A and B electrodes. A current is injected into the ground three times closing the circuit AC, BC and AB. The potential difference between M and N is measured in each case. Instead of increasing the current electrode spacing, like in Schlumberger soundings, all electrodes except C are moved along the profile. Resistivity values are calculated at each point for the three cases. The head-on profiling method is described by Flóvenz (1984).

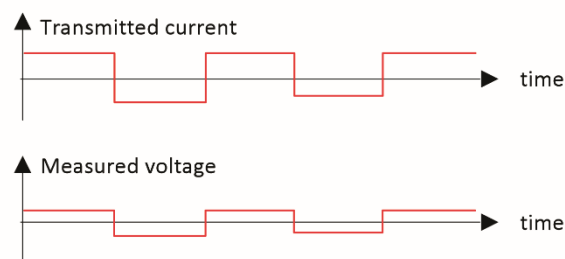


FIGURE 2: The setup of a Schlumberger sounding measurement (Flóvenz et al., 2012)

2.5.4 EM-methods

MT and AMT are natural source electromagnetic methods. AMT (audio-electromagnetics) refers to audio frequencies between 100 and 10 kHz. TEM is a controlled-source electromagnetic method (central loop and grounded dipole).

TEM (transient electromagnetic) method.

The TEM method is an active method used widely in geothermal exploration in Iceland. A constant current is injected into a transmitter loop from a transmitter that is fed by a generator or batteries. According to Biot-Savart's law, a constant magnetic field of known strength is created (Figure 3).

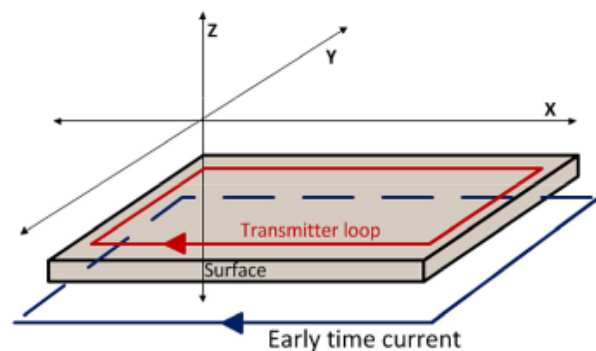


FIGURE 3: Current propagation at early times (from Badilla, 2011; modified from Rowland, 2002)

A receiver loop (big flexible loop or small coil) is connected to the receiver and placed at the centre of the transmitter loop. Then the current is abruptly turned off. The current and magnetic field decrease downwards and outwards and the magnetic field induces a current in the ground simultaneously in the resistive media that the current travels through at late times. (Figure 4).

After the turn off (the current turns off linearly) measurements start. During the decay of the magnetic field, a current is induced in the ground. According to Faraday's law, induced voltage in the receiver coil creates a decaying secondary magnetic field. The rate and magnitude of the decaying secondary magnetic field depends on the resistivity of the ground. Resistivity of the ground can be estimated by measuring the voltage that is registered in the receiver coil. Measurements are done in the big flexible loop (effective area of 57,000 m²) and a small loop (effective area of 100 m²) using a frequency of 2.5 and 25 Hz, respectively. The current and frequency are fed by the operator into the equipment. The turn off time is written down in the field book together with other information. Generally, the source loop is 200 × 200 m square and the transmitted current is 20-25 A.

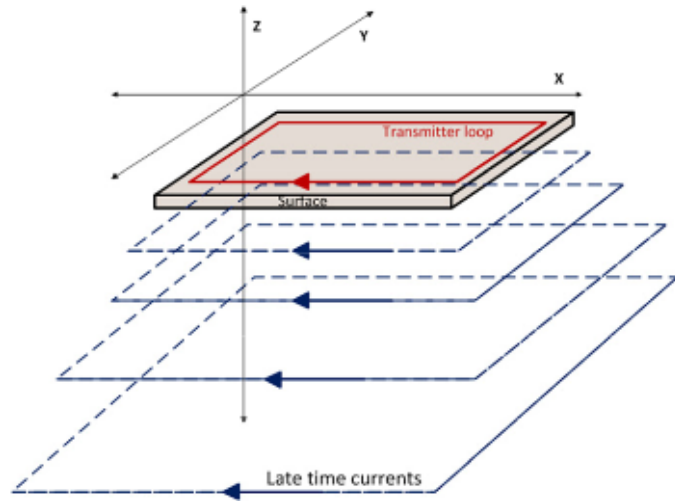


FIGURE 4: Current propagation at late times (from Badilla, 2011; modified from Rowland, 2002)

The depth of penetration of the TEM method depends on the resistivity beneath the sounding as well as on the setup geometry, the generated current and its frequency. The depth of penetration increases with time after the current turn-off (Flóvenz et al., 2012). The depth of penetration in the central loop TEM sounding depends on how long the induction in the receiver coil can be traced before it is drowned in noise. The induced voltage in the receiver coil in a homogeneous half space of conductivity σ at late time is given as (Árnason, 1989):

$$V(t, r) = I_0 \frac{C (\mu_0 \sigma r^2)^{3/2}}{10\pi^{1/2} t^{5/2}} \quad (17)$$

where, $C = A_r n_r A_s n_s \frac{\mu_0}{2\pi r^3}$;

- n_r = Number of windings in the receiver coil;
- A_s = Area of the transmitting loop (m²);
- A_r = Area of the receiver coil (m²);
- n_s = Number of windings in transmitting loop;
- t = Time elapsed after the current in the transmitter is turned off (s);
- μ_0 = Magnetic permeability in vacuum (Henry/m);
- $V(t, r)$ = Induced voltage (V);
- r = Radius of the transmitter loop (m);
- I_0 = Current in the transmitting loop (A).

The apparent resistivity can be derived from Equation 17:

$$\rho_a = \frac{\mu_0}{4\pi} \left[\frac{2I_0 \mu_0 A_r A_s n_r n_s}{5t^2 V(t, r)} \right]^{\frac{2}{3}} \quad (18)$$

Using Equation 18, the apparent resistivity curve is calculated as a function of time after the current is turned off.

MT (magnetotelluric) method

MT is a passive electromagnetic method that uses the natural magnetic field which provides a broad range of frequency between 10⁻⁴ and 10³ Hz. The magnetic field changes with time and a corresponding

electric field changes in the surface of the ground is measured to reveal subsurface resistivity distribution for great depth ranges. The signal sources are natural fluctuations of the Earth's magnetic field. Those fluctuations or primary magnetic field (H_p) induce a current in the ground (Kearey et al., 2002). A local conductive structure effects the density and distribution of the eddy currents. The current induces a secondary magnetic field (H_s). The resulting magnetic field $H = (H_p + H_s)$ is measured with induction coils in horizontal and orthogonal directions (H_x , H_y and H_z). The accompanied electric field (E_x and E_y) using a voltmeter as a potential difference ΔU between pairs of electrodes at distance L at the surface $\mathbf{E} = \Delta U/L$. The small amplitude geomagnetic time variations of the Earth's field contain a wide spectrum, generated by two different sources. One is a low frequency signal (< 1 Hz, long period) which is created from ionospheric and magnetospheric currents caused by solar winds radiating from the sun and interacting with the earth's magnetic field known as micropulsations. This is used for deep crustal and upper mantle structure investigations. The other one is high frequency (> 1 Hz, short period) signal that is generated by thunderstorm activity near the equator, used for shallow crustal structure study. The magnetic \mathbf{H} and electric field \mathbf{E} are measured at the surface and reveal the apparent resistivity ρ_a as a function of ω ($2\pi/T$).

$$\mathbf{E}(\omega) = \mathbf{Z}(\omega)\mathbf{H}(\omega) \quad (19)$$

where \mathbf{Z} is a tensor that depends on the resistivity structure of the ground and ω is the angular frequency (Hz) (Hersir and Björnsson, 1991).

The tensor equation can be written as:

$$\begin{bmatrix} E_x \\ E_y \end{bmatrix} = \begin{bmatrix} Z_{xx} & Z_{xy} \\ Z_{yx} & Z_{yy} \end{bmatrix} \begin{bmatrix} H_x \\ H_y \end{bmatrix} \quad (20)$$

For a 1D earth, conductivity changes with depth only. Therefore, the diagonal elements of the impedance tensors, Z_{xx} and Z_{yy} , are equal to zero, while the off-diagonal components are equal in magnitude, but have opposite signs:

$$Z_{xy} = -Z_{yx} \quad (21)$$

From the impedances, the apparent resistivity of the earth ρ_a and phase θ_a for each period T are calculated by the following relationships:

$$\rho_{xy}(T) = 0.2T|Z_{xy}|^2 = 0.2T \left| \frac{E_x}{H_y} \right|^2; \quad \theta_{xy} = \arg(Z_{xy}) \quad (22)$$

$$\rho_{yx}(T) = 0.2T|Z_{yx}|^2 = 0.2T \left| \frac{E_y}{H_x} \right|^2; \quad \theta_{yx} = \arg(Z_{yx}) \quad (23)$$

As mentioned above, $Z_{xy} = -Z_{yx}$, for a homogeneous and 1D Earth as well as $\rho_{xy} = \rho_{yx}$ (Flóvenz et al., 2012). In the 1D inversion in this work, the determinant of the impedance tensor, which is rotationally invariant (the value of the resistivity does not change with rotation) are used. The determinant value is calculated by the following equation:

$$\rho_{det} = \frac{1}{\omega\mu_0} |Z_{det}|^2 = \frac{1}{\omega\mu_0} \left| \sqrt{Z_{xx}Z_{yy} - Z_{xy}Z_{yx}} \right|^2; \quad \theta_{det} = \arg(Z_{det}) \quad (24)$$

The determinant of the impedance tensor is like an average value of the apparent resistivity (see Figure 10).

Skin depth is determined as a depth where the electromagnetic fields have been reduced to e^{-1} of their original value at the surface. It is used like a scale length for the time changing field or an estimate of how deep such a wave penetrates into the earth.

$$\delta = 500\sqrt{\rho T} \quad (25)$$

where δ = Skin depth (m);
 T = Period (s);
 ρ = Resistivity (Ωm).

The skin depth depends on the resistivity and the period. Consequently, a low frequency signal penetrates deeper into the earth than the high frequency signal (Hersir and Björnsson, 1991).

Static shift. All resistivity methods that measure the electric field on the surface suffer the static shift or telluric shift problem that is manifested as an unknown multiplier of the apparent resistivity. In MT, the electrical field ($E = \rho j$) is measured at the surface. It is affected by current distortion and topography. When voltage difference is registered on the surface and there is a high-resistivity body in the layer, the current always flows through the low-resistivity part. It causes a distortion of current, assuming that the current flows along the horizontal layers. Because of the shape of the topography, at high elevation, current density is low and the curve is shifted downwards but at the low elevation, it would be high and it is shifted upwards.

Static shift problems of MT are fixed by comparing the MT data with a nearby TEM resistivity curve when doing joint inversion. The TEM method is only sensitive to the near-surface resistivity structure and topography at early times. On the other hand the TEM data collected are measured during late times.

3. TEM AND MT DATA ACQUISITION

3.1 TEM data acquisition

In central loop TEM soundings, the transmitter is fed by a generator or batteries and connected with a transmitter loop, which is usually a square with a variable effective area of 40,000-90,000 m² (but rarely less than 10,000 m², except for shallower probing). Around 20–25 A current is injected from the transmitter into the transmitter loop. Additionally, even if the current is less than 10 A, one can get data with lower signal-to-noise ratio (SNR). The receiver is connected with the receiver loop that is a 10 × 10 m square loop with several windings and a circular loop of 1 m² with 100 windings (effective area is 100 m²), respectively. Those receiver loops are used at 2.5 Hz while a small loop is used at 25 Hz or even higher frequency. The receiver loop is placed at the centre of the transmitter loop.

Initially, the TEM receiver instrument is calibrated using a known signal source. Geonics PROTEM digital receiver can do its calibration automatically (Geonics, 1999). Time synchronization between the receiver and transmitter must be done precisely before the measurements are carried out because TEM works with very rapid signal transition. There are two ways to do synchronization, either through a reference cable or crystal clocks, which were used in this case.

3.2 MT data acquisition

In MT measurement, two lines are placed perpendicular to each other for the purpose of measuring the electric field (E_x and E_y) oriented N-S and E-W. The lines are connected to a data logger and an electrode that is usually composed of lead-chloride with a porous ceramic bottom for measuring telluric currents. The electrode must be in good contact with the ground. Magnetic coils are used to measure the magnetic field in three orthogonal directions (H_x , H_y and H_z). MT measurement setup is sketched in Figure 5.

For a homogeneous or layered earth, the electrical field is induced by its orthogonal source magnetic field (E_x correlates with H_y and E_y with H_x) (Hersir et al., 2013). In order to prevent noise from random or unnecessary movements, the coils are embedded into the ground. The polarity of the coils must be taken into account (Phoenix Geophysics, 2009). After the setup is completed, one should write down the direction of the setup and the coils used for each line and the distance between electrodes, as this information is needed for later data processing. The data logger is configured to record at least for one day. During night time the signal strength is stronger than during day time (Simpson and Bahr, 2005). Before the operator downloads the data from the MT units for processing, an MT data quality check has to be carried out at the site location. Example of time series data is shown in Figure 6. Data in Figure 6 are from the study presented here. The time series data are viewed by time series viewer.

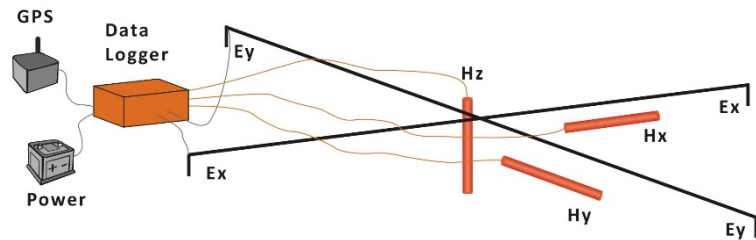


FIGURE 5: The setup of an MT sounding: Electrodes for measuring the electric field, coils for the magnetic field, acquisition unit for digital recording and GPS for synchronizing the data (Flóvenz et al., 2012)

each line and the distance between electrodes, as this information is needed for later data processing. The data logger is configured to record at least for one day. During night time the signal strength is stronger than during day time (Simpson and Bahr, 2005). Before the operator downloads the data from the MT units for processing, an MT data quality check has to be carried out at the site location. Example of time series data is shown in Figure 6. Data in Figure 6 are from the study presented here. The time series data are viewed by time series viewer.

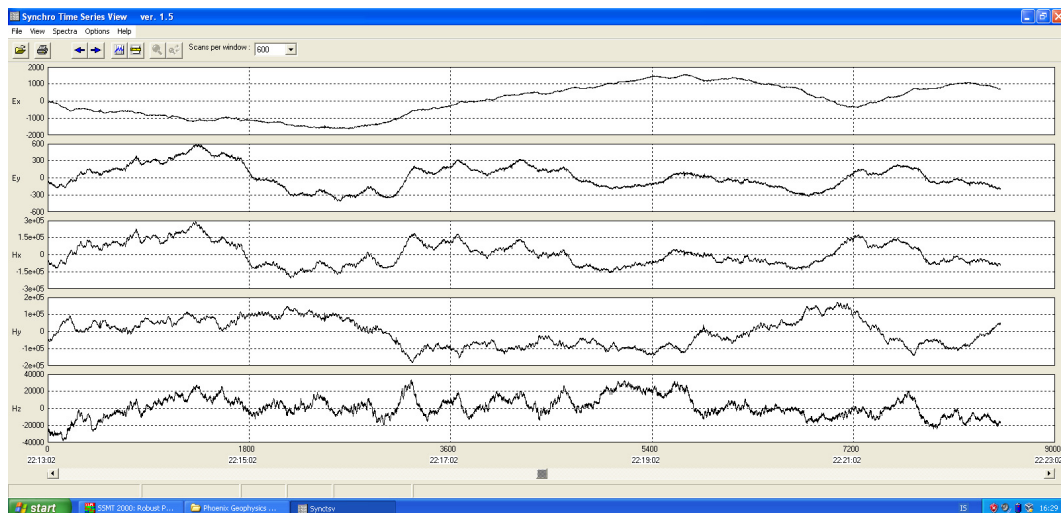


FIGURE 6: Time series data recording

4. PROCESSING OF TEM AND MT DATA

4.1 TEM data processing

TEM raw data are (extension .fru) files, which contain the induced voltage values measured during the late times in 20 gates (Figure 7) in the TEM receiver for different frequencies (25 Hz and 2.5 Hz). The raw data are an input for TemX (Árnason, 2006a) which is a Linux-based software. It supports stacking of the measured values and excludes outliers. The format of the output file is a text file (extension .inv) that includes the apparent resistivity. During one period one can measure 2 times and for the 25 Hz frequency one will have 50 measurements that are stacked in the program and for 2.5 Hz frequency, 5 measurements are stacked.

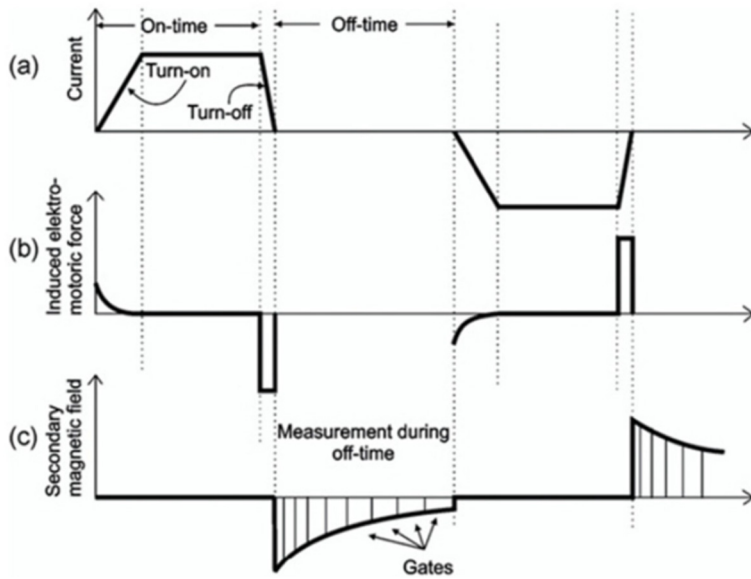


FIGURE 7: Time gates (Gichira, 2012)

4.2 MT data processing

Raw MT data are time series data that contain two electric and three magnetic field readings. Data processing is completed by SSMT2000 software provided by Phoenix Geophysics in Canada. The Fourier transform in its various forms, decomposes a time series data into its frequency components. In MT, raw time series data are processed using calibration and site parameter files. The Fourier coefficients are calculated and then reprocessed with data from base stations, using robust routines. The output MT plot file contains multiple cross powers for each of the frequencies analysed (Africa, 2013).

MTEditor is used for iterative weighting of residuals to identify and exclude data points. Finally, the resistivity and phase curves are plotted. Now we have data that is Fourier transformed and with misfit minimized. Then, there are some parameters of the plot files, which are displayed such as tipper magnitude, coherency between channels, and strike direction (shown in Figure 12 later). These files are converted into industry-standard Electrical Data Interchange (edi) format (SEG, 1991) for the TEMTD (Árnason, 2006b).

5. INVERSION OF THE DATA

The inversion problem consists of obtaining physical parameters that can explain the measured values. Modelling of resistivity soundings is achieved using forward modelling and, thereafter, an inversion process. In forward modelling, an apparent resistivity curve is calculated from a guessed initial model by the geophysicist. After the forward calculation, the measured and the calculated data are compared. Then, the model is changed and the process repeated until the best solution is found. Inversion works with data and the initial model to calculate the best solution of the forward calculation. The initial model is gradually enhanced through an iterative process by calculating adjustments to the model from the difference between the measured data and the response of the model (Figure 8), until a satisfactory fit is reached.

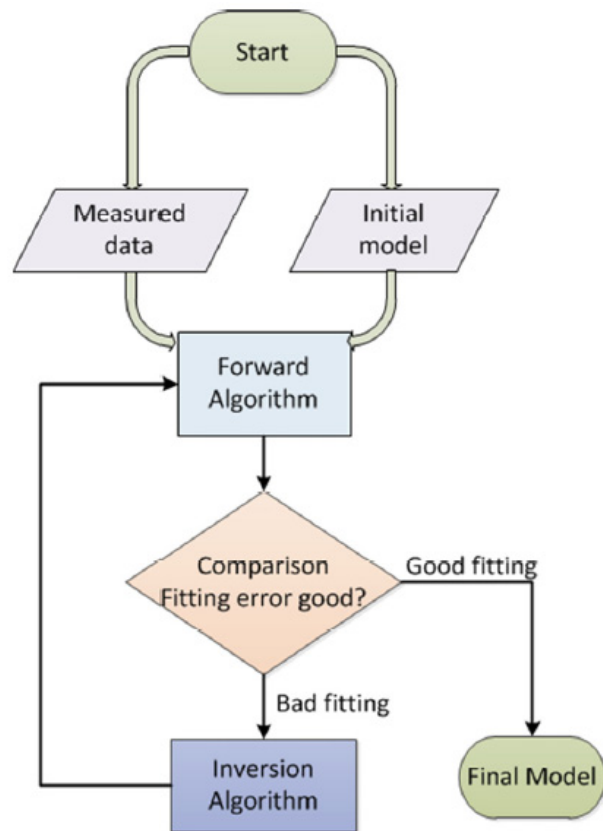


FIGURE 8: The inversion process

6. CASE EXAMPLE – EYJAFJÖRDUR LOW-TEMPERATURE AREA, N-ICELAND

6.1 The study area

Iceland lies at the intersection of the Mid-Atlantic Ridge and the Wyville-Thomson Ridge, a seismically inactive transverse ridge crossing most of the north-eastern branch of the North Atlantic between East Greenland and the Faroe Islands. The North America and Eurasian plate boundary crosses Iceland from southwest to northeast. Active volcanoes and earthquakes are signs of the plate boundaries in Iceland, showing where active plate movement is taking place. Productivity of volcanic material has been shown to be anomalously high on this part of the mid-oceanic ridge system (Vogt, 1971).

Eyjafjörður is the longest fjord in Iceland. It is located in the central north of the country (Flóvenz and Karlsdóttir, 2000). This is the second most populous area of Iceland with the town of Akureyri in its centre with almost 20,000 inhabitants. The mountains of Eyjafjörður are built of 3-10 m.y. old Tertiary volcanic formations. The rocks are mainly basaltic lavas with thin scoriaceous and sedimentary inter-layers. The lava pile dips about 4-7°C to the south and southeast. Thick sedimentary beds are found locally. At least three extinct central volcanoes are buried in the basaltic lava pile around Eyjafjörður (see Figure 9). Map of the Eyjafjörður area is presented in Figure 10 with locations of the TEM and MT soundings.

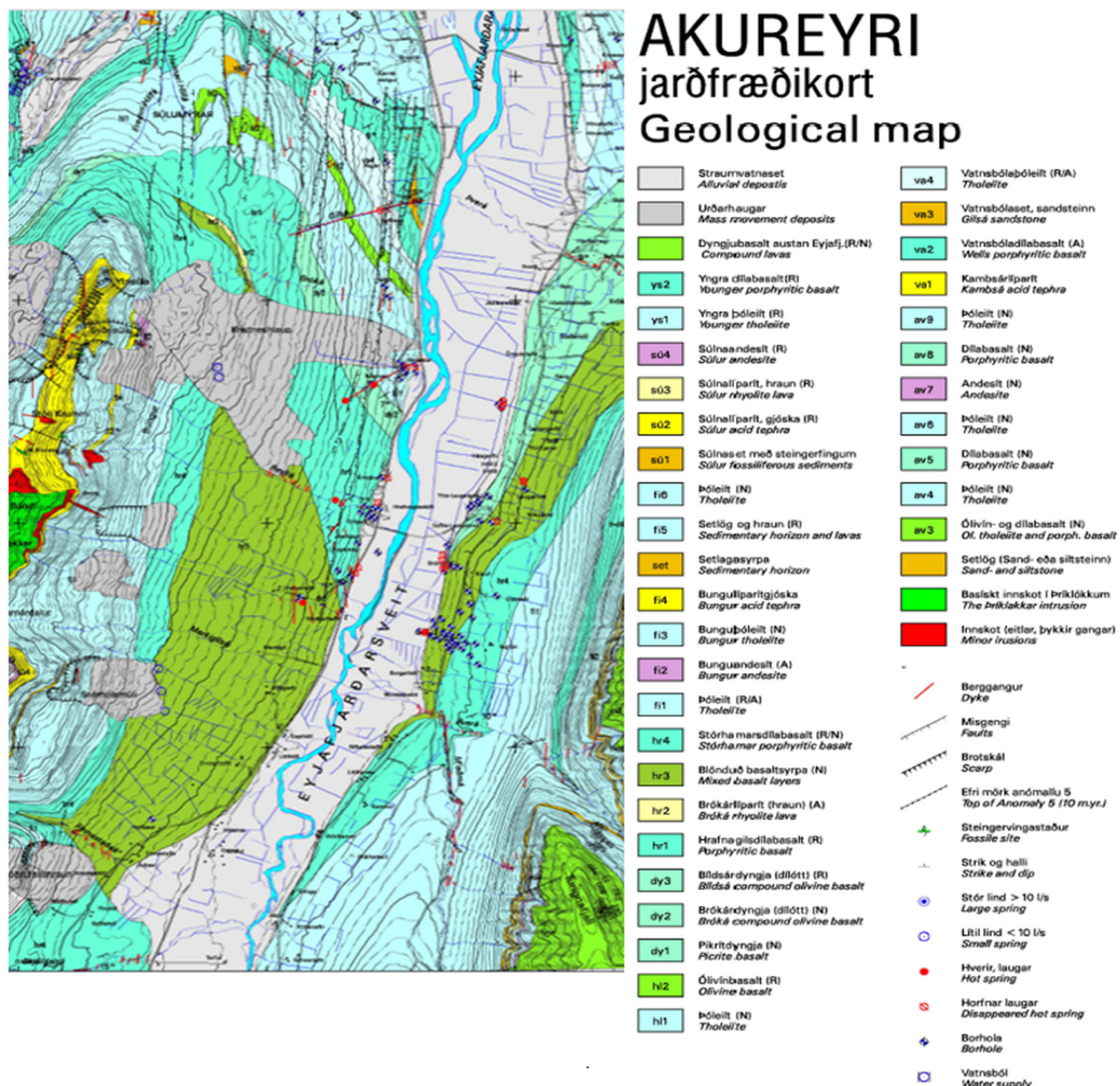


FIGURE 9: Geological map of the Eyjafjörður area (Hjartarson and Jónsdóttir, 2004)

6.2 TEM and MT soundings – data collection and processing

In framework of this work, 38 TEM soundings and 25 MT soundings are processed and inverted separately. Twenty-three of them are used here for the joint inversion (Figure 10). The stretched 2 lines shown in Figure 10 are locations of the resistivity cross-sections which were drawn down to different depths (see further Section 7.1).

6.2.1 1D inversion of TEM data

Input files for the inversion program, TEMTD (Árnason, 2006b) are .inv files that contain the apparent resistivity and a guessed model of resistivity and layer-thickness values using a layered model. The purpose of the inversion is to obtain the true resistivity for each layer. The output file includes resistivity changes with depth (Figure 11). The inversion algorithm that is used in the program is the non-linear least-squares inversion of the Levenberg-Marquardt type (Árnason, 2006b). The misfit function is the root-mean-square difference between measured and calculated values, weighted by the standard deviation of the measured values. In Occam inversion, which is used here in the inversion, layer thicknesses are kept fixed, equally spaced on a log scale, and the conductivity distribution is forced to be smooth by adjusting damping parameters. Appendix I shows the TEM data and the associated 1D models (Lkhagvasuren, 2016).

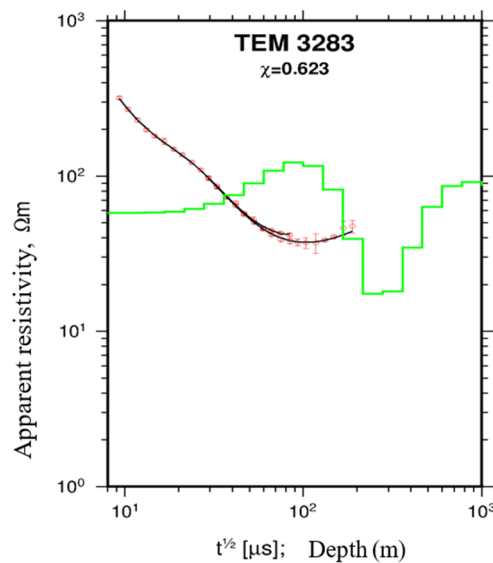


FIGURE 11: Inversion of TEM sounding 3283

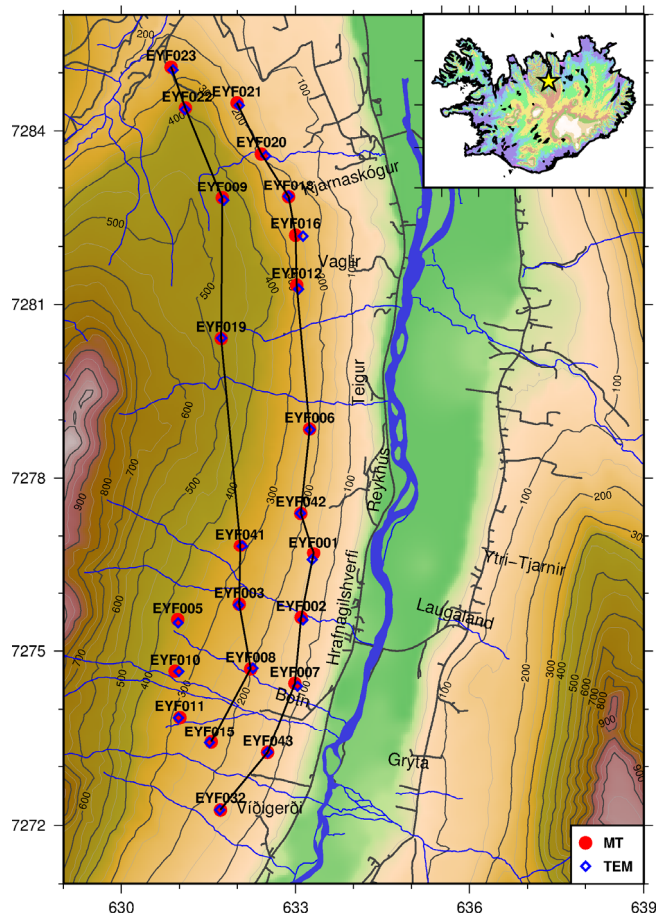


FIGURE 10: Location map for the TEM and MT soundings in Eyjafjörður. The yellow star on the Icelandic map on the right top corner of the figure shows the location of Eyjafjörður low-temperature geothermal area; locations of two cross-sections are shown as black lines

6.2.2 1D inversion of MT data

The magnetotelluric sounding method for the determination of subsurface electrical conductivity was first proposed by Cagniard (1953). For an an-isotropic or laterally inhomogeneous earth, the impedance becomes a tensor quantity. For the inversion program, the input is .edi-files from the MT soundings that include impedances or apparent resistivity and phase values. In the 1D case, only the determinant of the impedance tensor is used which is rotationally invariant. Figure 12 presents the apparent resistivity and phase derived from the xy (red) and yx (blue) components of the impedance tensor and the determinant invariant (black), the Z-strike or Swift angle (black dots), and multiple coherency of xy (red) and yx (blue) and ellipticity (gray dots). Appendix II shows the MT data and the associated 1D models (Lkhagvasuren, 2016).

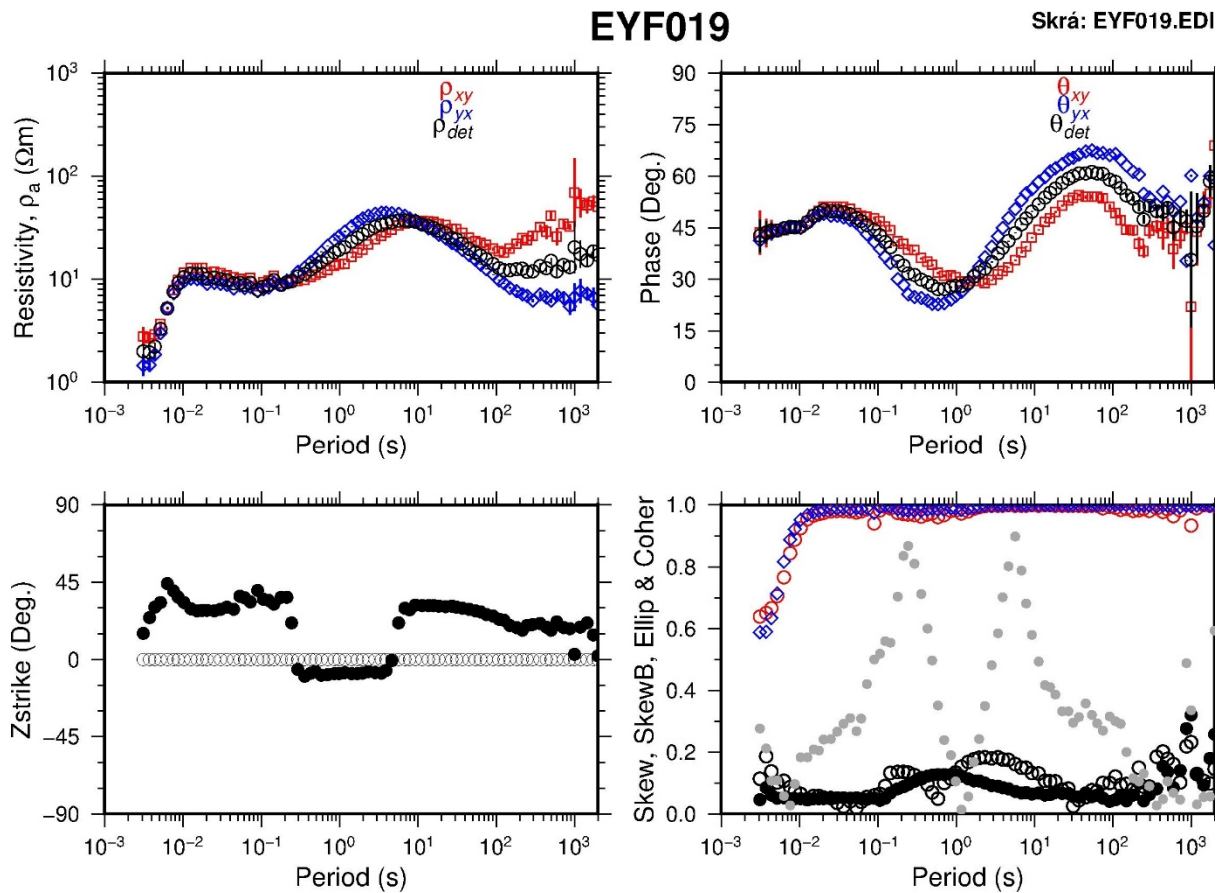


FIGURE 12: Processed data for MT sounding 019 from the Eyjafjörður low-temperature geothermal area, North Iceland

6.3 Joint 1D inversion of TEM and MT data

For the joint inversion, the input is .inv files for the TEM data and .edi files for the MT data. Joint inversion of TEM and MT data is executed using the TEMTD program. For 1D inversion of TEM data the program inverts for time, voltage and the apparent resistivity. The software is used to invert for the MT apparent resistivity and phase obtained from the rotationally invariant determinant of the tensor elements.

TEM soundings play an important role in correcting for static shift problem of MT data by jointly inverting both TEM and MT data. An example of the result of the jointly inverted TEM and MT data is presented in Figure 13.

Appendix III shows the 1D models of the joint inversion for all of the TEM and MT data (Lkhagvasuren, 2016).

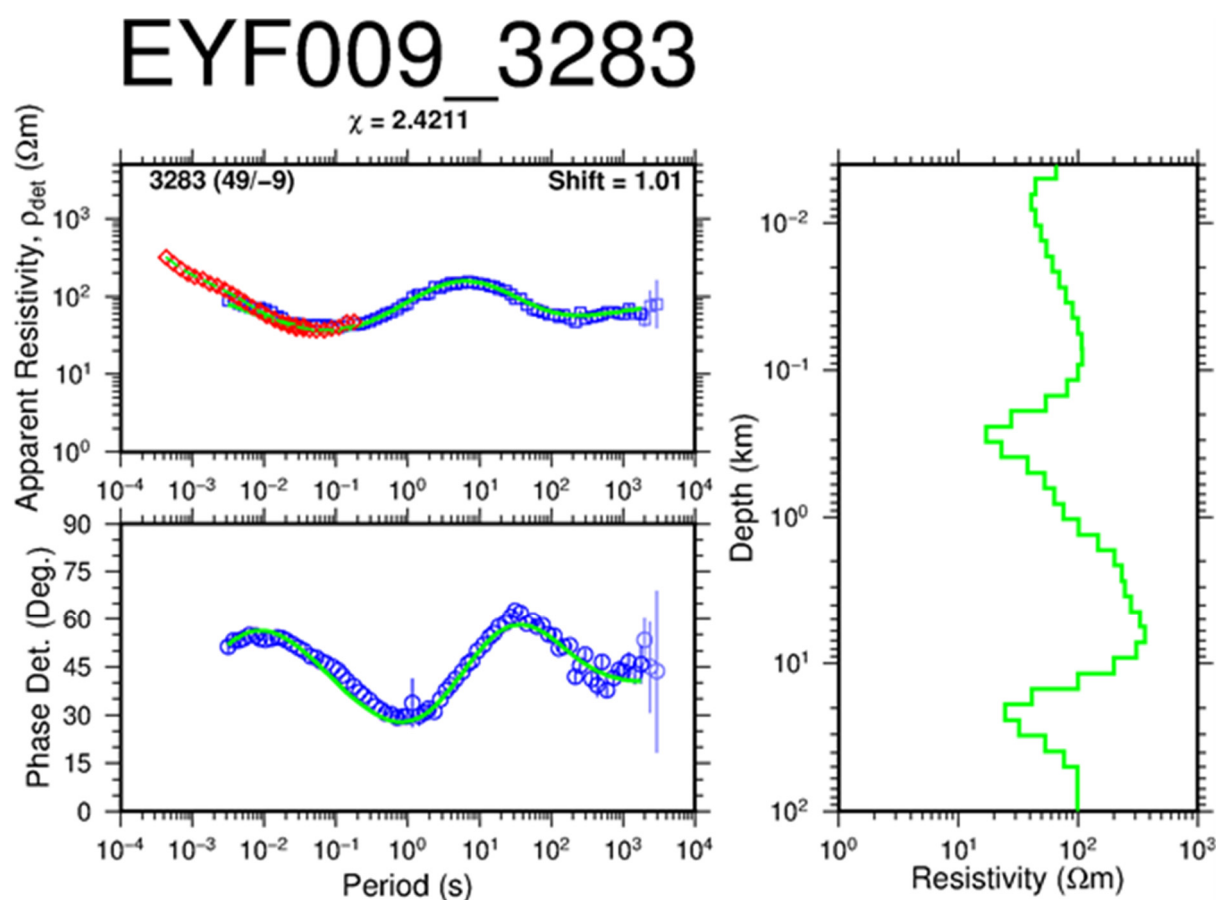


FIGURE 13: 1D joint inversion result of TEM sounding (3283) and MT sounding (EYF009); here, red diamonds are TEM apparent resistivity points, blue squares are MT apparent resistivity and blue circles are MT apparent phase points which are derived from the determinant of MT impedance tensor, green lines on the right represent the 1D joint inversion model. On top of the figure are the names of the MT and TEM soundings that are located close to each other and the misfit value. The shift value executed to MT data in order to fit the TEM data is 1.01

7. RESULTS

7.1 Resistivity cross-sections and resistivity depth slices

Figures 14 and 15 show two resistivity cross-sections reaching down to different depths in the Eyjafjörður area, based on the 1D joint inversion of the TEM and MT data. Additional cross-sections (down to different depths) are presented in Appendix 4 (Lkhagvasuren, 2016). Their location is given in Figure 10. A total of 8 resistivity depth slices are shown in Figures 16 and 17. Additional depth slices are shown in Appendix 4 (Lkhagvasuren, 2016).

The resistivity cross-sections show a shallow low-resistivity anomaly extending from the surface down to a depth of around 1,000 m. The low-resistivity is dipping upwards towards the north. At greater depths of several km, another low-resistivity body is seen in both cross-sections doming up in the northern part of the sections. These resistivity structures are even more visible in the depth slices. The deep lying conductive body is seen in one sounding only in the northwest part of the survey area at 7,000 and 10,000 m b.s.l. but extends over the northern part of the area at 15,000 m b.s.l. and in particular at 20,000 m b.s.l.

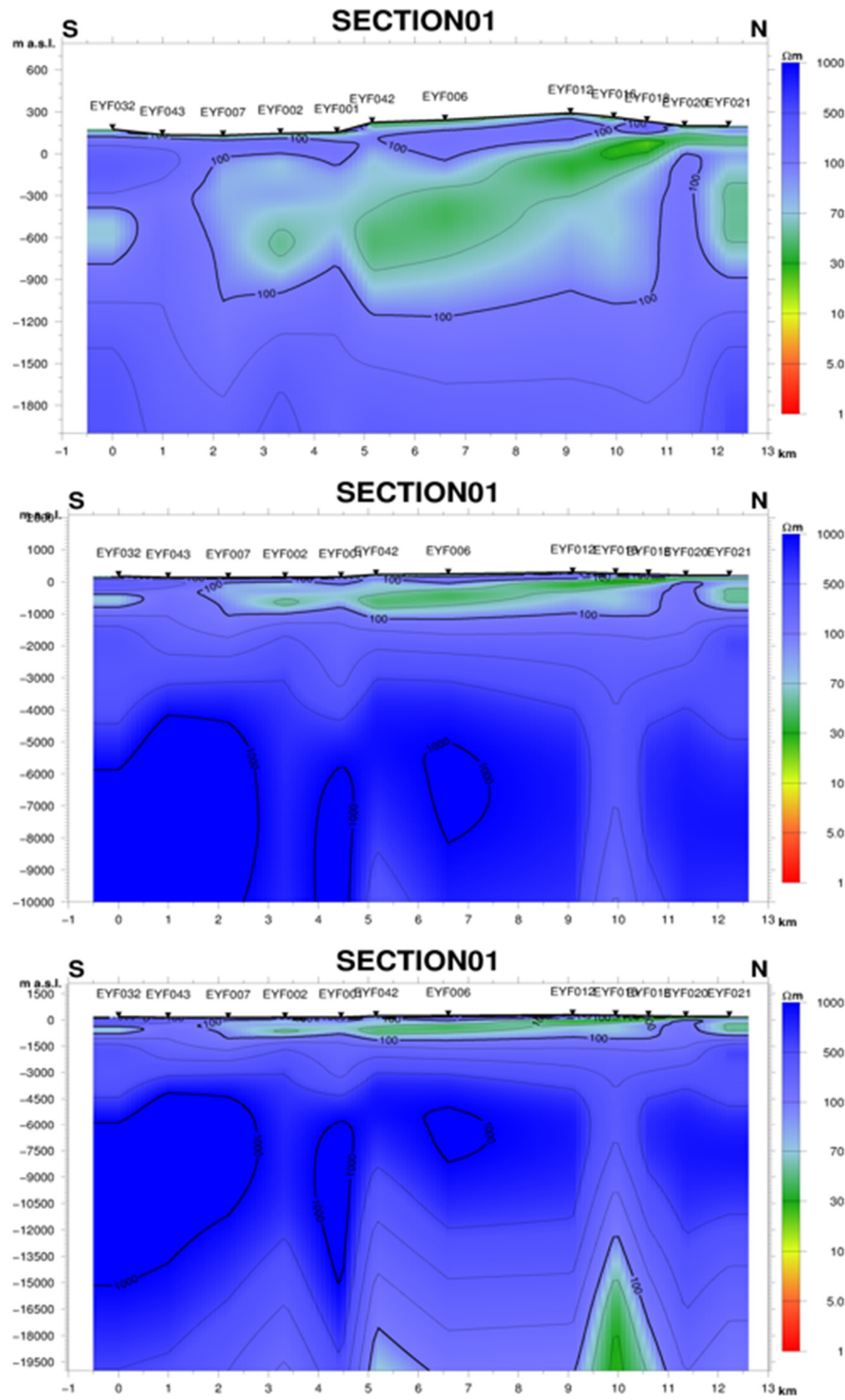


FIGURE 14: Resistivity cross-section N01 down to three depth levels, 2,000, 10,000 and 20,000 m b.s.l.; black triangles show the location of the MT soundings; the location of the cross-section is given in Figure 10

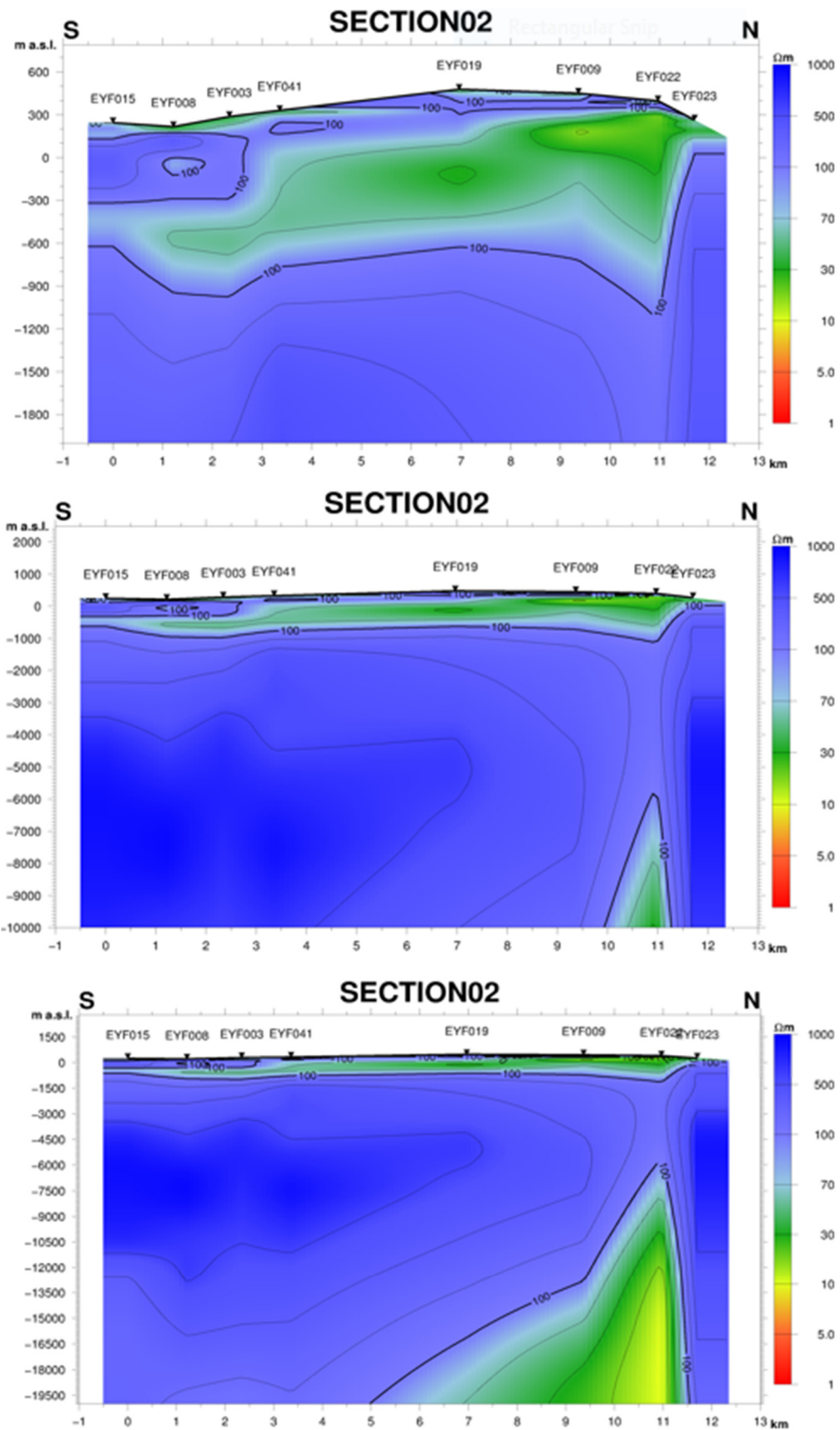


FIGURE 15: Resistivity cross-section N02 down to three depth levels, 2,000, 10,000 and 20,000 m b.s.l.; black triangles show the location of the MT soundings; the location of the cross-section is given in Figure 10

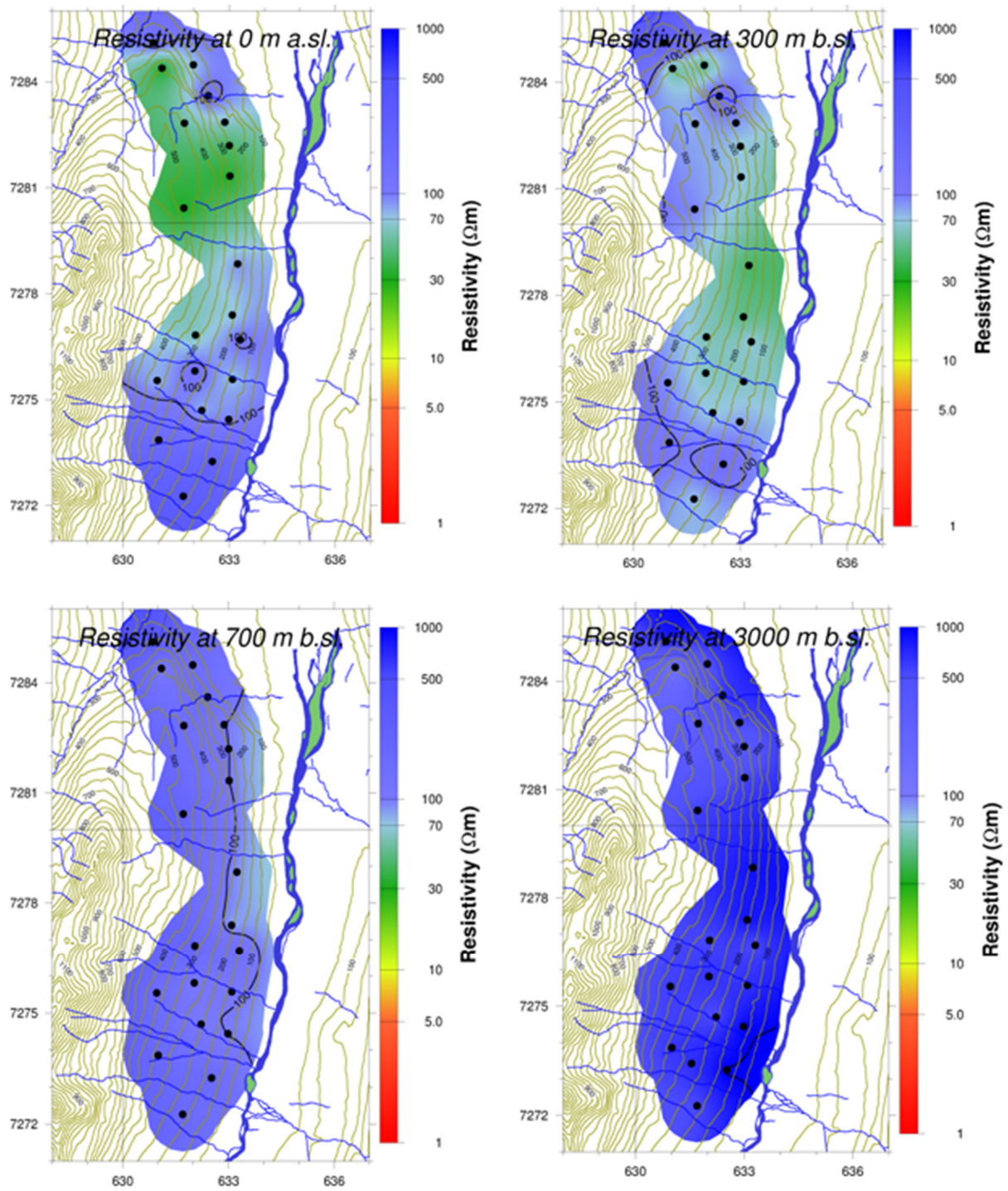


FIGURE 16: Resistivity depth slices at sea-level and at depths of 300, 700 and 3000 m b.s.l.; black dots show locations of MT soundings

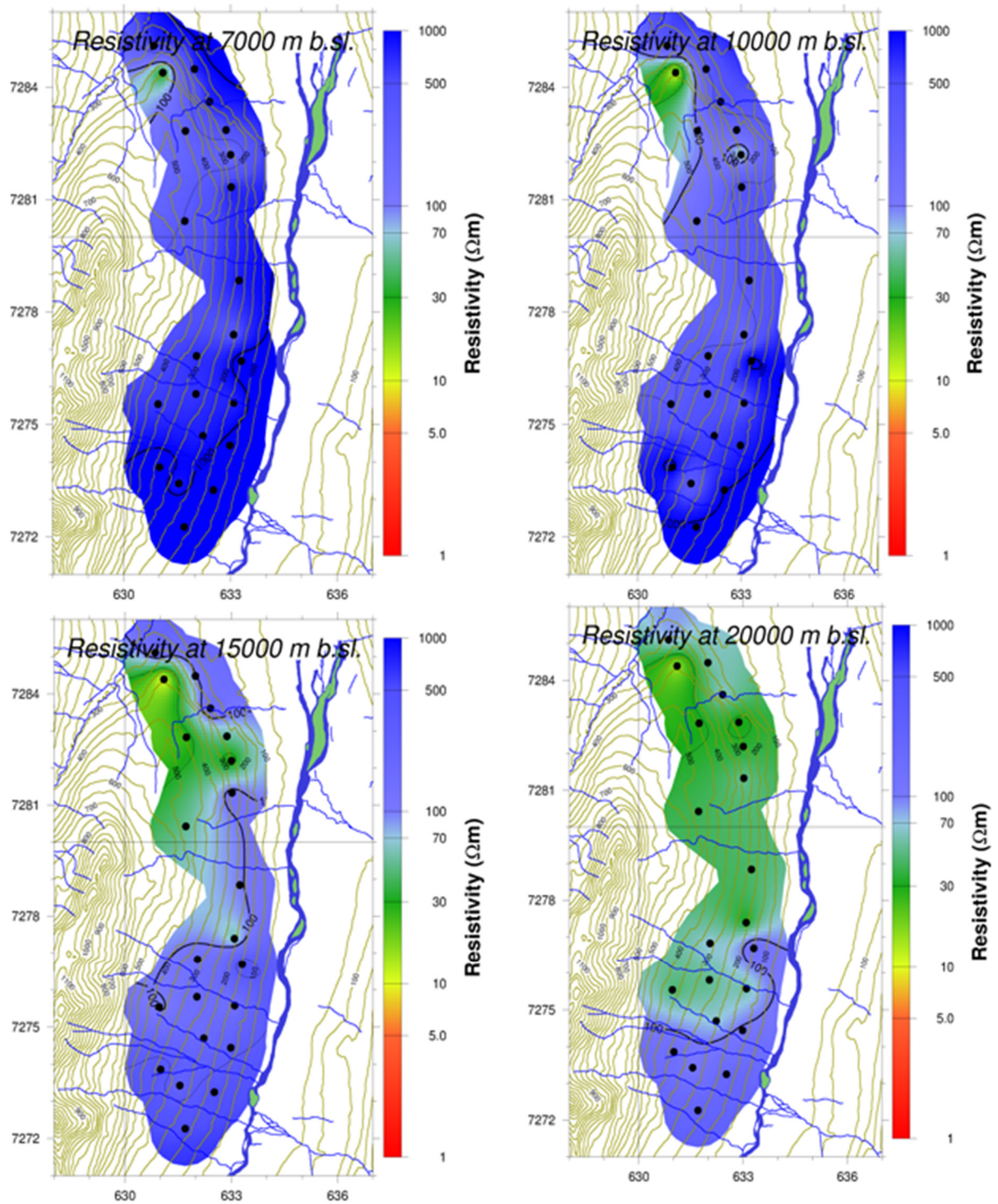


FIGURE 17: Resistivity depth slices at depths of 7,000, 10,000, 15,000 and 20,000 m b.s.l.; black dots show locations of MT soundings

8. CONCLUSIONS

Geophysical methods are mostly used in combination with other investigations. Here, a case study was done in Eyjafjörður low- temperature geothermal field where TEM and MT methods were applied. The TEM and MT data have been processed and 1D inverted. The 1D joint inversion of TEM and MT data was performed using the TEMTD inversion program. The resistivity depth slices and cross-sections have been mapped from the results of the joint inversion.

A resistivity cross-section along the same N-S profile has been done previously by Flóvenz and Karlsdóttir (2000) and compared with isotherms from deep boreholes in the south part of the cross-section (Figure 18). From a depth of around 300-800 m, a low-resistivity layer extends up to the surface along the dipping lava pile layers. To the left, a shallow lying low-resistivity anomaly is coinciding with a porphyritic and tholeiitic lava interbedded with sedimentary layers, a higher-resistivity layer coincides with a series of compound tholeiitic lavas. The low-resistivity anomaly observed in this work coincides with the temperature anomaly, which is interpreted as the main up flow zone of the geothermal activity according to Flóvenz and Karlsdóttir (2000). From the resistivity cross-sections and depth slices, a low-resistivity layer is seen extend upwards in a northerly direction. It reaches the surface at 11.5 km in cross-section 02 at 200 m a.s.l. (Figure 15).

A deep laying low resistivity is seen in cross-section 02 at 6,000 m b.s.l. and at 12,000 m in cross-section 01. It is seen in the subsurface in Eyjafjörður low-temperature area as in most of Iceland. It is presumably somehow connected to the heat source. According to Flóvenz and Karlsdóttir (2000), the heat source is

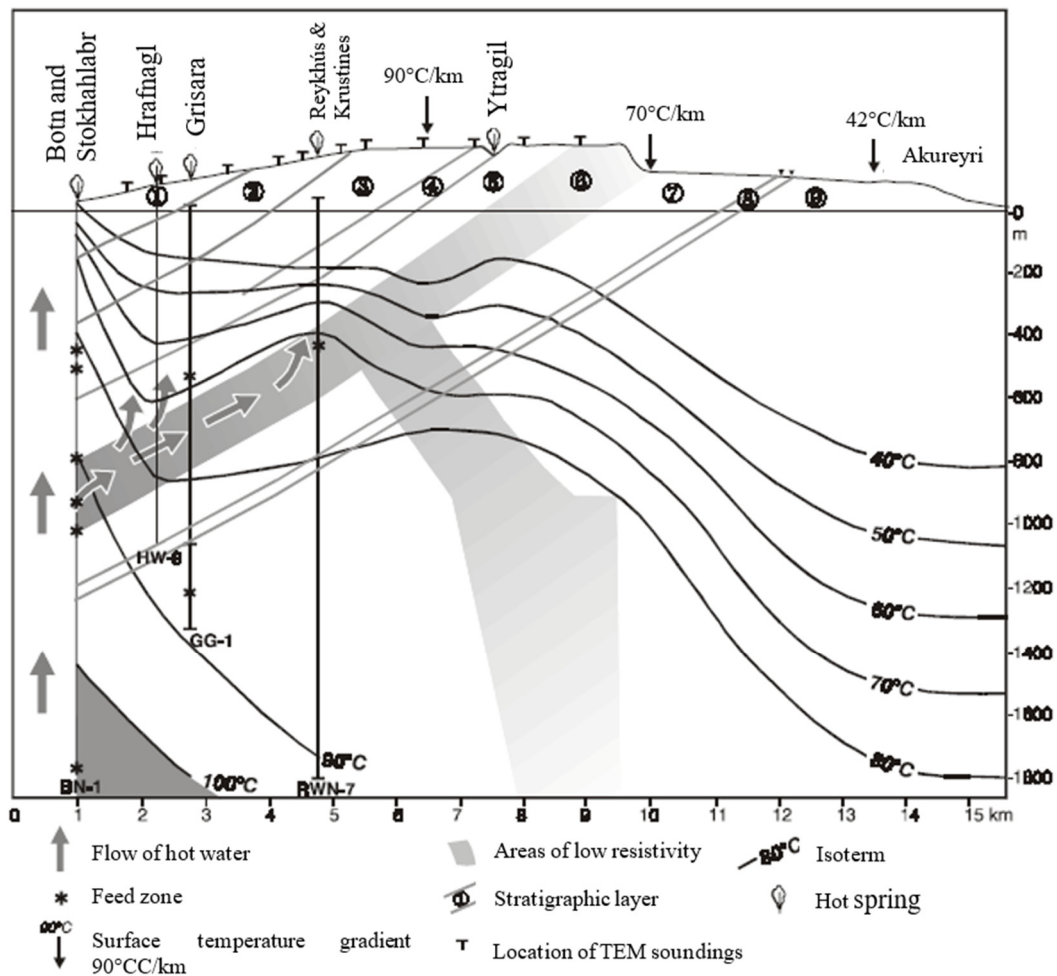


FIGURE 18: Geothermal interpretation of the Eyjafjörður low-temperature geothermal area (Flóvenz and Karlsdóttir, 2000)

around Botn area, close to MT soundings 007 and 008 (see Figure 10). When the results of this study are compared with those from Flóvenz and Karlsdóttir (2000), they are quite similar.

The low-resistivity anomaly is composed of porphyritic lavas, which temperature measurement analyses have shown to be the main up flow zone of the geothermal activity. The higher-resistivity host rock is presumably composed of a series of compound basaltic lavas.

Using resistivity surveying methods, the resistivity structure of the subsurface of the Earth is mapped as a function of depth. In geothermal areas, resistivity is prone to the parameters that can reveal the character of the geothermal reservoir. Resistivity surveying on the surface can directly probe deep structures in the subsurface of the Earth. It has many attributes for predicting the conditions of the geothermal reservoir. The main significance of resistivity surveying is diagnostic of geothermal activity and it adds to the understanding of geothermal reality in the subsurface.

ACKNOWLEDGEMENTS

I would like to appreciate my supervisors Mr. Gylfi Páll Hersir and Mr. Knútur Árnason for their support, kind discussions, direct advice and for revising the report. Also, I would like to express my gratitude to the UNU-GTP staff for their assistance and guidance during the past 6 months. I learned a lot of things during the 6 months of the geothermal training programme.

Thank you, dear international friends. I did not have time to get bored with you around. We were learning a lot, running, swimming, hiking and travelling to new places around Iceland where it is magnificent and peaceful.

I extend my appreciation to Demberel S (Director of Institute of Astronomy and Geophysics in Mongolia) for this big opportunity to learn and to my colleagues for their assistance and encouragement. I thank my whole family for taking care of our boys. It was obviously a big support for the study and work not to have to worry about the kids.

Also I want to express my appreciation to ÍSOR staff for their kind help.

REFERENCES

Africa, J.R., 2013: 1D inversion of MT and TEM data with application of soundings from Krýsuvík, SW-Iceland and a review of MT/TEM data from Bacman geothermal project, Central Philippines. Report 5 in: *Geothermal training in Iceland 2013*. UNU-GTP, Iceland, 1-34.

Archie, G.E., 1942: The electrical resistivity log as an aid in determining some reservoir characteristics. *Tran. AIME*, 146, 54-67.

Árnason, K., 1989: *Central-loop transient electromagnetic sounding over a horizontally layered earth*. Orkustofnun, Reykjavík, report OS-89032/JHD-06, 129 pp.

Árnason, K., 2006a: *TemX short manual*. ÍSOR – Iceland GeoSurvey, Reykjavík, report, 17 pp.

Árnason, K., 2006b: *TEMTD (Program for 1D inversion of central-loop TEM and MT data)*. ISOR – Iceland GeoSurvey, Reykjavík, short manual 16 pp.

- Badilla E., D., 2011: Resistivity imaging of the Santa Maria sector and the Northern zone of Las Pailas geothermal area, Costa Rica, using joint 1D inversion of TDEM and MT data. Report 8 in: *Geothermal training in Iceland 2011*. UNU-GTP, Iceland, 85-118.
- Burger, H.R., Sheehan, A.F., and Jones, C.H., 2006: *Introduction to applied geophysics*. W.W. Norton & Company, Inc., NY, 614 pp.
- Cagniard, L., 1953: Basic theory of the magneto-telluric method of geophysical prospecting. *Geophysics*, 18, 605-635.
- Dakhnov, V.N., 1962: Geophysical well logging. *Q. Colorado Sch. Mines*, 57-2, 445 pp.
- Flóvenz, Ó.G., 1984: Application of the head-on resistivity profiling method in geothermal exploration. *Geothermal Resources Council. Transactions*, 8, 493-498.
- Flóvenz, Ó.G., Hersir, G.P., Saemundsson, K., Ármannsson, H., and Fridriksson Th., 2012: Geothermal energy exploration techniques. In: Sayigh, A. (ed.), *Comprehensive renewable energy*, vol. 7. Elsevier, Oxford, 51-95.
- Flóvenz Ó.G., and Karlsdóttir, R., 2000: TEM-resistivity image of a geothermal field in N-Iceland and the relation of the resistivity with lithology and temperature. *Proceedings of the World Geothermal Conference 2000, Kyushu – Tohoku, Japan*, 1127-1132.
- Geonics, Ltd., 1999: *Operating manual for PROTEM 67 D*. Geonics Ltd, Ontario, 58 pp.
- Georgsson, L.S., 2009: Geophysical methods used in geothermal exploration. *Presented at Short Course IV on Exploration for Geothermal Resources, organized by UNU-GTP, KenGen and GDC, at Lake Naivasha, Kenya*, UNU-GTP, SC-10, 16 pp.
- Georgsson, L.S., and Karlsdóttir, R., 2007: Resistivity methods – DC and TEM with examples and comparison from the Reykjanes peninsula and Öxarfjörður, Iceland. *Paper presented at “Short Course II on Surface Exploration for Geothermal Resources”, organized by UNU-GTP and KenGen, at Lake Naivasha, Kenya*, UNU-GTP SC-5, 14 pp.
- Gichira, J.M., 2012: Joint 1D inversion of MT and TEM data from Menengai geothermal field, Kenya. Report 11 in: *Geothermal training in Iceland 2012*. UNU-GTP, Iceland, 137-167.
- Hersir, G.P., and Árnason K., 2009: Resistivity of rocks. *Paper presented at “Short Course on Surface Exploration for Geothermal Resources”, organized by UNU-GTP and LaGeo, Santa Tecla, El Salvador*, UNU-GTP SC-09, 8 pp.
- Hersir, G.P., and Björnsson, A., 1991: *Geophysical exploration for geothermal resources. Principles and applications*. UNU-GTP, Iceland, report 15, 94 pp.
- Hersir, G.P., Vilhjálmsson, A.M., and Árnason K., 2013: 3D inversion of magnetotelluric (MT) resistivity data from Krýsuvík high temperature geothermal area in SW Iceland. *Proceedings of the 38th Workshop on Geothermal Reservoir Engineering, Stanford University, Stanford, CA*, 14 pp.
- Hjartarson, Á., and Jónsdóttir, H.E., 2004: *Akureyri, geological map* (2. ed.). ÍSOR – Iceland GeoSurvey, Reykjavík.
- Kearey, P., Brooks, M., and Hill, I., 2002: *An introduction to geophysical exploration*. Blackwell Scientific Publications, Oxford, 254 pp.

Kulhanek, O., 1988: *Anatomy of seismogram*. Elsevier, Amsterdam, 178 pp.

Lee L., K., Lerner, B.W., and Cengage, G., 2006: *Porosity and permeability*. World of Earth Science, webpage: www.enotes.com/earth-science/.

Lichoro, C.M., 2014: Gravity and magnetic methods. *Presented at Short Course IX on Exploration for Geothermal Resources, organized by UNU-GTP, GDC and KenGen, at Lake Bogoria and Lake Naivasha, Kenya*, UNU-GTP SC-19, 8 pp.

Lkhagvasuren, S., 2016: *Appendices to the report "Resistivity surveying in geothermal exploration with an application to the Eyjafjörður low-temperature area, N-Iceland"*. UNU-GTP, Iceland, report 25 appendices, 41 pp.

Lucius, J.E., Langer, W.H., and Ellefsen, K.J., 2006: *An introduction to using surface geophysics to characterize sand and gravel deposits*. US Geological Survey, Reston, VI, open-file report 2006-1257, 55 pp.

Mariita N.O., 2011: Application of geophysical methods to geothermal energy exploration in Kenya. *Presented at Short Course VI on Exploration for Geothermal Resources, organized by UNU-GTP, GDC and KenGen, at Lake Bogoria and Lake Naivasha, Kenya*, UNU-GTP SC-13, 9 pp.

Phoenix Geophysics, 2009: *Data processing. User's guide*. Phoenix Geophysics, Ltd., Toronto.

Rowland, B.F., 2002: *Time-domain electromagnetic exploration*. Northwest Geophysical Associates, Inc., report, 6 pp.

Samaranayake, S.A., 2015: Seismic monitoring of geothermal fields: A case study of Hellisheidi geothermal field. Report 32 in: *Geothermal training in Iceland 2015*. UNU-GTP, Iceland, 727-754.

SEG, 1991: *MT/EMAP data interchange standard*. Society of Exploration Geophysicists, 112 pp.

Simpson, F., and Bahr, K., 2005: *Practical magnetotellurics*. Cambridge University Press, Cambridge, UK, 254 pp.

Todd, D.K., and Mays, L.W., 2005: *Groundwater hydrology* (3rd ed.). John Wiley & Sons, Inc., NY, 636 pp.

Vogt, P.R., 1971: Asthenosphere motion recorded by the ocean floor south of Iceland. *Earth Planet. Sci. Lett.*, 13, 153-160.